PHYSICAL REVIEW LETTERS

X-Ray Microprobe of Orbital Alignment in Strong-Field Ionized Atoms

L. Young,* D. A. Arms, E. M. Dufresne, R. W. Dunford, D. L. Ederer, C. Höhr, E. P. Kanter, B. Krässig, E. C. Landahl,
E. R. Peterson, J. Rudati, R. Santra, and S. H. Southworth

Argonne National Laboratory, Argonne, Illinois 60439, USA

We have developed a synchrotron-based, time-resolved x-ray microprobe to investigate optical strong-field processes at intermediate intensities (10^{14}–10^{15} W/cm^2). This quantum-state specific probe has enabled the direct observation of orbital alignment in the residual ion produced by strong-field ionization of krypton atoms via resonant, polarized x-ray absorption. We found strong alignment to persist for a period long compared to the spin-orbit coupling time scale (6.2 fs). The observed degree of alignment can be explained by models that incorporate spin-orbit coupling. The methodology is applicable to a wide range of problems.

PACS numbers: 42.50.Hz, 32.80.Rm, 41.60.Ap

Studies of atoms in the gas phase subjected to moderately intense laser fields (10^{14}–10^{15} W/cm^2) have led to the discovery of phenomena with significant fundamental and technological interest [1]. A prominent example is that of high-order harmonic generation (HHG), where recent advances have produced coherent, ultrafast soft x-ray radiation [2,3], pulses of attosecond duration [4,5] and enabled the imaging of molecular orbitals [6]. The high-order harmonic radiation is generated by simply focusing an optical laser in a gas target. The dynamics within a single atom can be described semiclassically in three steps [7,8]. A valence electron tunnels through the laser-suppressed Coulomb barrier; the freed electron propagates in the laser field; electron recombination with the residual ion produces high-order harmonic radiation. While the main features of the HHG process have been explained using this simple model, both the nonperturbative single atom response and the propagation of the high-order harmonic radiation through the complex plasma medium present theoretical challenges. Tour-de-force efforts [2] yield a 10^{-10} conversion efficiency to high-order harmonics in a 10% bandwidth around the carbon K edge. For progress, a theory with quantitative predictive power is desirable, but has so far remained elusive [9].

Experimental information for comparison to theory is limited at the gas densities used for HHG because of the plasma conditions. Earlier studies of the atomic response to strong-laser fields concentrated on the detection of ejected particles (photons, electrons, ions) from the volume defined by the focused laser beam. At low densities, both traditional [10] and sophisticated multicoincidence methods [11] have been used to detect ions and electrons emerging from an isolated event. At higher densities (10^{17}–10^{19}/cm^3) used for HHG [2,3] a transient plasma is formed and a quantitative interpretation of charged particle yields or electron energy and angular distributions becomes problematic. The properties of the target medium are deduced through simulation and subsequent comparison to the measured high-harmonic output [2].

Here we report three advances: (1) development of an *in situ* x-ray probe of optical strong-field processes capable of interrogating atoms in a transient dense plasma environment, (2) direct observation of orbital hole alignment resulting from strong-field ionization, and (3) demonstration of the importance of atomic spin-orbit coupling for understanding the degree of alignment.

Understanding orbital alignment in the residual ion formed by strong-field ionization is a basic, but essentially unexplored issue. Usually it is assumed that in the presence of a strong-laser field the laser polarization provides a quantization axis and m_l, m_s quantum numbers are conserved. Because the electron tunneling rate is strongly dependent on the m_l sublevel, ion alignment can occur during the ionization process [12,13]. For $|m_l| = 1$ sublevels, the ionization rate can be an order of magnitude lower than for $m_l = 0$. Specifically, Taïeb and co-workers [14] calculate for strong-field ionization to Kr$^+$ an $m_l = 0$ population of 95%. To our knowledge, only one experiment—at ultrastrong laser intensities (10^{16}–10^{18} W/cm^2)—has explored this issue [15], albeit indirectly. Gubbini *et al.* [15] measured ion yields as a function of laser intensity and compared to predictions of Ammosov-Delone-Krainov [12] tunneling formula to obtain a measure of the degree of ion alignment. No alignment was observed. Here we demonstrate a more direct and quantitative probe of orbital alignment using resonant polarized x-ray absorption and observe orbital alignment.

We introduce a micron-sized x-ray probe into the high-field volume generated in a laser focus. Tunable x rays enable ion spectroscopy in this extreme environment. The x-ray absorption spectrum of Kr$^+$ contains a distinct, essentially background-free signature, i.e., the $1s \rightarrow 4p$ resonance that is absent in neutral Kr due to the filled $4p$ shell. Since x-ray absorption addresses unoccupied orbitals according to dipole selection rules, the polarized x rays are a direct probe of orbital alignment in the residual ion. Although the x-ray pulse duration of the synchrotron (100 ps) is long relative to that of the laser (40 fs), it is

still short enough to probe the residual ions as they are produced within a localized volume and initially have thermal velocity, ~300 nm/ns. Hard x rays are essential because they readily penetrate the plasma environment and produce a prompt, collision-free response via x-ray fluorescence following K-shell excitation. Inner-shell lifetimes are subfemtosecond and x-ray interaction cross sections are small (10^{-21} cm^2) relative to charged particle interaction cross sections (10^{-16} cm^2). Because of these considerations and the relatively large interparticle spacing in a gas, the measured x-ray absorption spectra are those of isolated atoms and ions [16].

Our experimental arrangement, shown in Fig. 1, incorporates the essential feature of microfocused x rays into a laser-pump–x-ray-probe configuration. The microfocus configuration represents a gain of 10^4 in tunable x-ray flux density over standard laser-pump–x-ray-probe experiments [17] enabling our gas phase experiments with only 10^7–10^9 atoms in the focal volume. [In comparison, typical laser-pump–x-ray-probe experiments on dilute solutions require concentrations of 1-mmol [17], corresponding to 10^{14} solute atoms in a typical 1-mm^3 volume.] Monochromatic 14.3 keV x rays from an undulator at Sector 7 of the Argonne Advanced Photon Source were efficiently focused by a large-aperture, dynamically bent Kirkpatrick-Baez mirror pair [18] to a FWHM of 10 μm (10^6 x rays/pulse, $\Delta E/E \sim 10^{-4}$, 271 kHz). The x rays probed the 100-micron FWHM focus of a regeneratively amplified Ti:sapphire laser (2.0 mJ, 40 fs, 800 nm, 1 kHz). Krypton atoms from a room temperature effusive gas jet were ionized by the laser and subsequently probed by the x rays as a function of time, space, x-ray energy, and polarization. An energy dispersive silicon-drift detector recorded the emitted x rays and a cylindrical mirror analyzer was used to measure ion and electron energy distributions. A 1-mm slit was placed between the interaction region and x-ray detector to define the viewing length along the optical propagation axis. We obtained a K edge absorption spectrum of the ionized atoms by recording the krypton $K\alpha$ fluorescence yield as a function of incident x-ray energy. Laser-on/laser-off spectra were acquired simultaneously by tagging each detected $K\alpha$ photon with its associated incident x-ray pulse which arrived either with or without a laser pulse. Because of the substantial mismatch
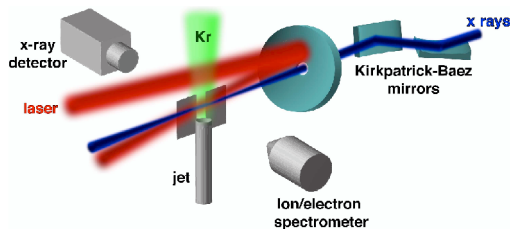
in laser and x-ray repetition rates coupled with the complex fill pattern of the synchrotron, only 1/3000 of the total x-ray flux is coincident with the laser.

The x-ray absorption spectra of neutral and ionized krypton are shown in the upper and lower panels of Fig. 2. The striking new feature is the strong resonance at 14.313 keV due to a vacant $4p$ orbital created by strong-field ionization at a peak on-axis intensity of 4×10^{14} W/cm^2. At this intensity it is impossible to create only a single charge state of Kr. Thus, the laser-on spectrum contained contributions from both Kr^{1+} and Kr^{2+} in addition to a neutral background. The laser-on spectrum was fit with three parameters, a neutral background and amplitudes for Kr^{1+} and Kr^{2+} (Kr:Kr^{1+}:Kr^{2+} = 0.44:0.41:0.14) with 10% uncertainty. The neutral background was determined by the laser-off spectrum. Theoretical spectra for the krypton ions were constructed by combining the discrete lines from *ab initio* relativistic configuration interaction calculations [19] with a continuum matching algorithm [20]. These theoretical spectra were convolved with the natural width of the K vacancy (2.7 eV) and the x-ray bandwidth (1.5 eV) for comparison with experimental data. The spectra reveal the shifting of the oscillator strength from the continuum to the discrete lines as a function of ionization stage as well as the change in the K-shell oscillator strength sum rule for higher Z atoms [21]. We note that the oscillator strength of the $4p$ resonance in Kr^{2+} is roughly twice that in Kr^{1+}, due to the presence of two holes in the $4p$ shell. At the $1s \rightarrow 4p$ resonance, the absorption cross section for the Kr^{1+} is 26 kb/atom compared to 0.5 kb/atom for the Kr neutral,
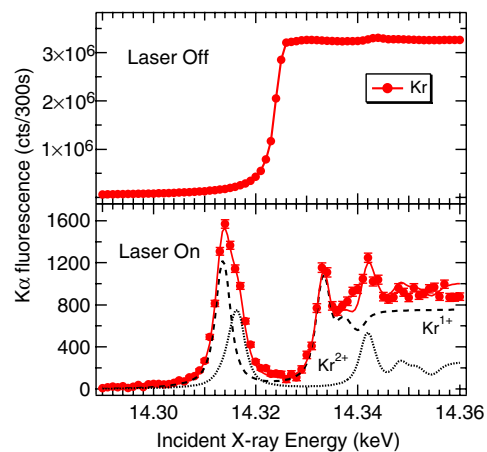
FIG. 2 (color online). Near K edge spectra of krypton. Top: fluorescence excitation near K edge spectrum of neutral krypton. Bottom: same for krypton ionized by a circularly polarized optical laser field. The neutral background has been subtracted. Dashed (dotted) line is the *ab initio* Kr^{1+} (Kr^{2+}) spectrum convolved with the experimental bandwidth. Solid line is the sum of the Kr^{1+} and Kr^{2+} components. The Kr^{1+}:Kr^{2+} ratio is ~3 within the localized viewing region.

FIG. 1 (color online). Microfocused x rays probe atoms in the focus of a high-intensity laser.

making the resonance an almost background-free monitor for Kr^{1+}.

The signature $1s \rightarrow 4p$ resonance is used to detect the alignment of the $4p$ orbital hole created in the initial strong-field ionization step. Making the standard assumption that the tunnel ionization is predominantly $m_l = 0$, then in the absence of perturbations, the vacated $4p$ orbital will remain fixed in space along the laser polarization axis, z. [The alternative multiphoton ionization picture also gives strongly preferential ionization of $m_l = 0$ as confirmed by nonrelativistic multiphoton ionization calculations we performed using the Floquet-type technique described in [22].] Thus, one would expect a strong absorption resonance for a probe polarization aligned parallel ($\parallel$) to the laser polarization. Conversely, with the x-ray probe polarized perpendicular ($\perp$) to the laser polarization, the $1s \rightarrow 4p$ resonance should be suppressed. For an $m_l = 0$ population of 95% [14], a $\parallel$: $\perp$ absorption ratio of 38:1 would be expected—if spin-orbit coupling is not taken into account.

We observed a $\parallel$: $\perp$ absorption ratio of 2.0:1, as shown in Fig. 3 for a peak intensity of 4×10^{14} W/cm^2 at a laser–x-ray delay of <1 ns [23]. The observed ratio is attained after verifying the polarization state (>99% linear) and optimizing laser–x-ray overlap. The 2:1 ratio appears only at the $1s \rightarrow 4p$ resonance; 1:1 is observed in the other regions of the near-edge x-ray absorption spectrum, including both higher Rydberg resonances in the ion and the continuum. Thus, no alignment is observed, as expected, except when the $4p$ hole orbital is probed. The 2:1 ratio is constant over a tenfold variation in gas density. Reducing the laser intensity by a factor of 7 causes the ratio to increase slightly to 2.4:1, a trend predicted by the models below.

Two simple models, which both include spin-orbit coupling, can explain the observed ratio. We consider pump and probe pulses that are longer than the $4p$ spin-orbit
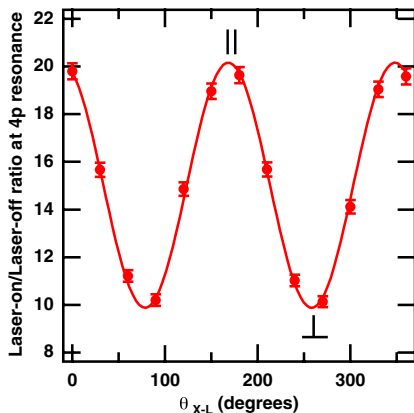

FIG. 3 (color online). Evidence of orbital alignment of strong-field ionized krypton. The laser-on/laser-off ratio of x-ray fluorescence yield at the $1s \rightarrow 4p$ resonance as a function of θ_{X-L}, the angle between laser and x-ray polarization directions.

period (6.2 fs). Model I follows the usual time-dependent picture starting with preferential ionization of $m_l = 0$ in a strong field. After passage of the laser pulse, the initial m_l distribution evolves into the spin-orbit coupled eigenstates of the $4p$ orbital hole $j = 3/2, 1/2, m_j = \pm 1/2$ in the ion. X-ray absorption then probes the distribution of these j, m_j states. To generalize, for arbitrary fractions ρ_0 and ρ_1 of the initially produced $m_l = 0$ and $|m_l| = 1$ states we derived a formula for the ratio of parallel-to-perpendicular absorption for the $1s \rightarrow 4p$ transition based upon standard angular momentum algebra and dipole selection rules [24].

$$R = \frac{10\rho_0 + 4\rho_1}{4\rho_0 + 7\rho_1}. \quad (1)$$

Inserting $\rho_0 = 95\%$, $\rho_1 = 5\%$ [14], we obtain $R = 2.3$, consistent with experiment.

Model II, also consistent with experimental observations, arises when one realizes that, in fact, the laser electric field is not strong enough to break the atomic spin-orbit coupling. Using an effective one-electron model of strong-field ionization that includes atomic spin-orbit coupling, we found that even at the electric-field strength corresponding to the saturation intensity for the ionization of Kr, there is very little mixing between the $4p_{3/2}$ and $4p_{1/2}$ orbitals. At an electric-field strength of 0.10 a.u. one state has a squared overlap with the field-free $4p_{1/2}$ state of 0.98 and the second has a squared overlap with the field-free $4p_{3/2}$ state of 0.96. This shows that the uncoupled m_l, m_s quantum numbers do not properly describe the Kr$^+$ states that are populated by strong-field ionization of krypton.

We derived the following equation for the $\parallel$: $\perp$ x-ray absorption ratio in terms of $\rho_{j,|m_j|}$, the probability of finding Kr$^+$ with a hole in either the $4p_j$, m_j or the $4p_j$, $-m_j$ states [24]. (All $\rho_{j,|m_j|}$ are non-negative and their sum equals 1.)

$$R = \frac{2\rho_{1/2,1/2} + 4\rho_{3/2,1/2}}{2\rho_{1/2,1/2} + \rho_{3/2,1/2} + 3\rho_{3/2,3/2}}. \quad (2)$$

We draw the following conclusions from this equation. First, the observable ratio can never be greater than 4. Second, using a rate equation approach, we find at the saturation intensity the Kr$^+$ state populations are $\rho_{3/2,1/2} = 69\%$, $\rho_{1/2,1/2} = 26\%$, and $\rho_{3/2,3/2} = 5\%$, which gives $R = 2.4$. Like model I, model II provides reasonable agreement with experiment. Note that the assumptions underlying model I predict a $\parallel$: $\perp$ x-ray absorption ratio of >10 at the moment of ionization. The two models might therefore be distinguished by experiments using ultrashort laser-pump–x-ray-probe pulses on the few fs time scale, which may soon become available with x-ray free-electron lasers [25].

The calculated ratio R [Eq. (2)] will be slightly overestimated if the ionization from the more strongly bound

$4p_{1/2}$ is underestimated. This is expected from a tunneling model, which does not account for the fact that at 800 nm the same number of photons are required to ionize both the $4p_{3/2}$ and $4p_{1/2}$. The tunneling model predicts that a decrease in laser intensity will suppress ionization from $4p_{1/2}$ and thus increase R, as observed experimentally. Finally, the effect of the presence of Kr^{2+} is not included in our model, which describes x-ray absorption to a single p orbital. In our measurements, the contribution from Kr^{2+} is expected to be small because the $4p$ resonance for the Kr^{2+} is shifted by 2.5 eV to higher x-ray energies and the fraction of Kr^{2+} is small.

The agreement between the models and experiment suggests that any laser-driven electron recollision process, which occurs at half the laser period of 2.8 fs, does not disturb the orbital alignment. The presence of the laser field during the recollision process may preserve alignment, as expected due to the cylindrical symmetry of the combined laser-atom system. In addition, no change in the degree of alignment is observed over a few hundred picoseconds which implies that collision-induced dealignment processes in the plasma are negligible on this time scale.

These findings have important implications for spectroscopy of laser-created ions. The discrete $1s \rightarrow 4p$ resonance may be significantly suppressed (a factor of 2) relative to the continuum, depending upon the relative orientation of the laser and x-ray polarizations. Our spectroscopic measurements presented in Fig. 2 were made with a circularly polarized laser and collinear x-ray beam and thus were insensitive to the relative orientations of the x-ray and laser polarizations.

The time-resolved x-ray microprobe has revealed orbital alignment in strong-field ionization, but many other applications exist as well. Of general interest is that the efficient use of laser power in the microfocus geometry will enable pump-probe studies of structural dynamics [17,26] at a variety of laser wavelengths with currently available laser sources. With stretched laser pulses that temporally overlap the x-ray pulses, one can study molecular alignment processes [27] and also the perturbation of an atomic near-edge spectrum due to the ponderomotive shift of the threshold [28]. The spectroscopic power of an x-ray microprobe combined with a powerful ultrafast laser can also provide new perspectives on laser-produced plasmas with controllable conditions [29] and anomalous x-ray propagation in dense plasmas [30]. Another logical extension is the study of strong-field processes at relativistic intensities, where unexplored physics of clusters [31] and individual atoms [14,15] are of interest.

*Electronic address: young@anl.gov
[1] T. Brabec and F. Krausz, Rev. Mod. Phys. **72**, 545 (2000).
[2] J. Seres *et al.*, Nature (London) **433**, 596 (2005).
[3] E. A. Gibson *et al.*, Science **302**, 95 (2003).
[4] M. Hentschel *et al.*, Nature (London) **414**, 509 (2001).
[5] P. Agostini and L. F. DiMauro, Rep. Prog. Phys. **67**, 813 (2004).
[6] J. Itatani *et al.*, Nature (London) **432**, 867 (2004).
[7] P. B. Corkum, Phys. Rev. Lett. **71**, 1994 (1993).
[8] M. Lewenstein *et al.*, Phys. Rev. A **49**, 2117 (1994).
[9] A. Gordon and F. X. Kärtner, Phys. Rev. Lett. **95**, 223901 (2005).
[10] R. R. Freeman and P. H. Bucksbaum, J. Phys. B **24**, 325 (1991).
[11] J. Ullrich *et al.*, Rep. Prog. Phys. **66**, 1463 (2003).
[12] M. V. Ammosov, N. B. Delone, and V. P. Krainov, Sov. Phys. JETP **64**, 1191 (1986).
[13] M. V. Frolov *et al.*, Phys. Rev. Lett. **91**, 053003 (2003).
[14] R. Taïeb, V. Véniard, and A. Maquet, Phys. Rev. Lett. **87**, 053002 (2001).
[15] E. Gubbini *et al.*, Phys. Rev. Lett. **94**, 053602 (2005).
[16] In addition to isolated atom properties, we have measured collective response, i.e., Coulomb expansion of the transient ion/electron ensemble (to be published).
[17] L. X. Chen *et al.*, Science **292**, 262 (2001).
[18] P. J. Eng *et al.*, Proc. SPIE Int. Soc. Opt. Eng. **3449**, 145 (1998).
[19] L. Pan, D. R. Beck, and S. M. O'Malley, J. Phys. B **38**, 3721 (2005).
[20] R. F. Reilman and S. T. Manson, Phys. Rev. A **18**, 2124 (1978).
[21] J. A. Wheeler and J. A. Bearden, Phys. Rev. **46**, 755 (1934).
[22] R. Santra and C. H. Greene, Phys. Rev. A **70**, 053401 (2004).
[23] The $\parallel : \perp$ absorption ratio changes on the few ns time scale due to ion/electron dealignment collisions (to be published).
[24] R. Santra *et al.* (to be published).
[25] P. Emma *et al.*, Phys. Rev. Lett. **92**, 074801 (2004).
[26] H. Ihee *et al.*, Science **309**, 1223 (2005).
[27] H. Stapelfeldt and T. Seideman, Rev. Mod. Phys. **75**, 543 (2003).
[28] M. D. Davidson *et al.*, Phys. Rev. Lett. **71**, 2192 (1993).
[29] N. H. Burnett and P. B. Corkum, J. Opt. Soc. Am. B **6**, 1195 (1989).
[30] J. Filevich *et al.*, Phys. Rev. Lett. **94**, 035005 (2005).
[31] T. Ditmire *et al.*, Nature (London) **386**, 54 (1997).